Journal of Optoelectronics and Advanced Materials Vol. 5, No. 1, March 2003, p. 157 - 169

INVITED PAPER

STRUCTURAL AND MAGNETIC INVESTIGATIONS OF TRANSITION METAL IONS IN TeO_2 BASED GLASSES

I. Ardelean*, S. Filip[a]

Faculty of Physics, Babes-Bolyai University, 3400 Cluj-Napoca, Romania
[a]Department of Physics, University of Oradea, 3700 Oradea, Romania

Electron paramagnetic resonance (EPR) and magnetic susceptibility measurements are performed on $xM_nO_m\cdot(100-x)[70TeO_2\cdot25B_2O_3\cdot5PbO]$ glasses with $M_nO_m \Rightarrow Cr_2O_3$ ($0 < x \leq 20$ mol %), Fe_2O_3 ($0 < x \leq 20$ mol %), MnO ($0 < x \leq 40$ mol %) or CuO ($0 < x \leq 40$ mol %). The EPR absorption spectra due to paramagnetic ions (Cr^{3+}, Fe^{3+}, Mn^{2+} and Cu^{2+}) in vitreous matrix revealed the structural details of the diamagnetic host, the coordination, distribution and valence states of the paramagnetic ions, the EPR parameters being sensitive to the local symmetry, the character of the chemical bonds, as well as to structural factors. EPR and magnetic susceptibility data have shown that the magnetic ions are present in the glasses as isolated species, coupled by dipole-dipole and negative superexchange interactions. The strength of interaction that involves magnetic ions was determined as a function of concentration and the valence states of magnetic-active ions were revealed. The particular behaviour of the transition metal ions in the glassy matrix depends on the nature and concentration of the paramagnetic ions.

(Received July 22, 2002; accepted March 12, 2003)

Keywords: TeO_2 based glass, ESR, Magnetic susceptibility

1. Introduction

Due to certain features of the behaviour of TeO_2 as glass-former and the interesting properties of tellurite glasses having a number of technical applications, the structural study of these vitreous matrices is imposed as very useful. Tellurite glasses are known as high-index optical glasses having a considerable infrared transmission [1]. They have applications as acousto-optical materials [2], as laser and photochromic glasses [3]. At the some time the TeO_2 plays an important role in the synthesis of glass-ceramics [4], porous glasses for ultra-filters [5] or materials used in optoelectronics [6].

The purpose of this paper is to present the EPR and magnetic susceptibility data and to show how these data succeed to give the image of the structure of tellurite glasses, by investigating the paramagnetic ions distributions inside the vitreous matrix in conection with various basic structural units. The studies were carried out on the system $70TeO_2\cdot25B_2O_3\cdot PbO$ containing chromium, iron, manganese and copper ions.

2. Experimental

The investigated systems: (1) - $xCr_2O_3\cdot(1-x)[70TeO_2\cdot25B_2O_3\cdot5PbO]$, (2) - $xFe_2O_3\cdot(1-x)[70TeO_2\cdot5B_2O_3\cdot5PbO]$, (3)- $xMnO\cdot(1-x)[70TeO_2\cdot25B_2O_3\cdot5PbO]$, (4)- $xCuO\cdot(1-x)[70TeO_2\cdot25B_2O_3\cdot5PbO]$ were obtained from starting materials TeO_2, H_3BO_3, PbO, Cr_2O_3, $MnCO_3$, Fe_2O_3 and respectively CuO of reagent grade purity. The samples were prepared by weighing the components in suitable

* Corresponding author: arde@phys.ubbcluj.ro

proportion, mixing the powders and melting these admixtures in sintered corundum crucibles. The temperatures and the melting conditions were the same: 1000 ^{o}C for 10 min, for all systems. The melt was poured onto stainless steel plates. The structure of the samples were studied by X-ray diffraction analysis and any crystalline phase was not revealed up to 20 mol% Cr_2O_3, 20 mol% Fe_2O_3, 40 mol% MnO, and respectively 40 mol% CuO.

The EPR measurements were performed at room temperature in X-band (9.4GHz) and 100 kHz field modulation with a JEOL-type equipment.

The magnetic susceptibility data were carried out with a Faraday-type balance, in the temperature range 80-300 K for the systems (1), (2) and (3). The magnetic measurements for the system (4) were performed with an Oxford Instrument-type balance, in the temperature range 4.2-200 K and fields, H, up to 80 kOe. In order to obtain the magnetic susceptibilities, at each temperature, χ values were determined from magnetisation isotherms by extrapolation of the experimental data to $H^{-1} \rightarrow 0$ [7].

3. Results and discussion

3.1. EPR and magnetic susceptibility studies of glasses from system (1)

A great variety of vitreous systems were investigated by means of Cr^{3+} EPR absorption spectra including glasses such as phosphate [8], borate [9], fluoride [10], borosulphate [11], bismuthate [12] and also chalcogenide [13]. In some oxide glasses Cr^{5+} species were also detected [14-16].

Fig. 1 shows the EPR absorption spectra due to Cr^{3+} ions for glasses from system (1). For all glasses the spectrum consists of low-field absorption centered at $g \approx 4.8$ and high field absorption centered at $g \approx 1.97$. The low-field absorption is a broadened one and extends from $g \approx 5.6$ to $g \approx 4.3$. The high-field absorption increase in intensity when the Cr_2O_3 content of the glasses rises up to 20 mol %. The line-width of the $g \approx 1.97$ absorption depends on sample composition and presents a complex evolution vs concentration (Fig. 2). After an increase for $x \leq 3$ mol %, the line-width decreases abruptly ($3 \leq x \leq 10$ mol %) and the increases again. These is a competition between broadening and narrowing effects on the EPR absorption line for samples containing $x > 3$ mol % of Cr_2O_3.

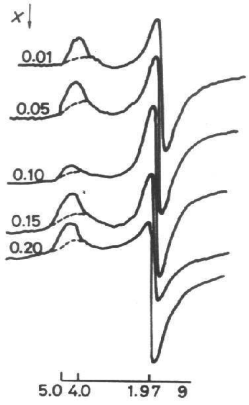

Fig. 1. EPR absorption spectra due to Cr^{3+} ions in glasses from system (1).

The low-field resonance is generally attributed to isolated Cr^{3+} ions in distorted sites due to strong ligand-field effects. These ions are subjected to a strong orthorhombic crystal field arising from a slightly distorted octahedral environment. Due to the crystalline field parameters distribution in glasses the absorption lines are broadened and often appear as a superposition of contributions. The low-field absorption in our spectra (Fig. 1) can be attributed to Cr^{3+} ions in strongly distorted sites with a symmetry predominantly rhombic, but there are slightly different axial distribution of the Cr^{3+}

ions vicinity besides the rhombic ones. Consequently, the absorption line is broadened because of the superposition of absorptions that have g_{eff} distribution. As background of the absorption centered at $g \approx 4.8$ there is another broad line absorption at $g \approx 4.0$ (approximated by the dotted line in Fig. 1) which can be attributed to sites with predominantly axial character. The low-field absorption of Cr^{3+} ions does not depend on the Cr_2O_3 content in the glasses. The isolated Cr^{3+} ions preserve their ability to order their vicinity in local structural units of a certain symmetry. This evolution of the matrix structure is not characteristic for the Cr^{3+} containing vitreous systems previously studied [14, 15].

The high-field absorption at $g \approx 1.97$ increases with the Cr_2O_3 content of the glasses. The line-width dependence (Fig. 2) shows the increase due to dipolar broadening up to x = 3 mol %. The absorption can be attributed to Cr^{3+} ions in slightly distorted octahedral symmetric sites involved in dipole-dipole type interactions. For x > 3 mol % the line-width increase is stopped by narrowing mechanisms due to exchange-type interactions. This balances the dipolar broadening, because the two mechanism affect, simultaneously, the Cr^{3+} ions. The exchange narrowing is efficient within $3 \leq x \leq 10$ mol %. For x > 10 mol % the magnetic interaction seems to be affected by the structural disordering of the glasses due to Cr^{3+} and the line broadens again. In contrast to Cr^{3+} in sites giving rise to the low-field absorptions, the local order around Cr^{3+} that enhances the absorptions at $g \approx 1.97$ is very sensitive to the progressive Cr^{3+} ions accumulation in the vitreous matrix.

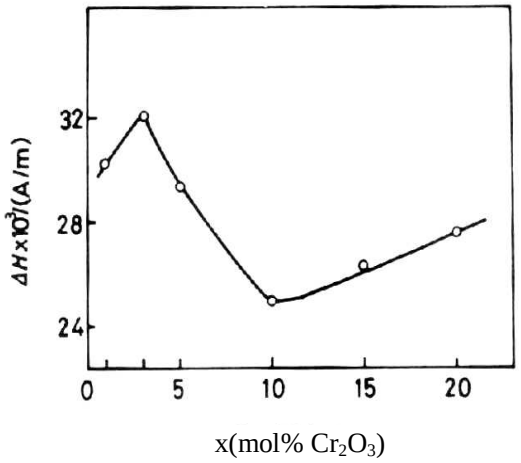

Fig. 2. The composition dependence of the line-width for $g \approx 1.97$ absorption.

The temperature dependence of the reciprocal magnetic susceptibility of these glasses is presented in Fig. 3. For glasses containing $x \leq 3$ mol % this dependence obeys a Curie law. For these compositions, as indicate the EPR data, the Cr^{3+} are isolated or subjected to dipole-dipole interactions. For compositions with x > 3 mol % dependences in Fig. 3 obeys a Curie-Weiss law, with negative paramagnetic temperature, θ_p. For these glasses the magnetic data indicates negative superexchange interactions between Cr^{3+} ions, which are predominantly antiferromagnetically coupled. In glasses the magnetic interactions are short-range ones, probably of mictomagnetic type [17]. These results agree with those obtained by means of EPR, revealing for x > 3 mol % most of Cr^{3+} ions as experiencing superexchange-type interactions, together with small concentrations of isolated ones. Similar data concerning Cr^{3+} doped oxide glasses were obtained by other authors [8, 12, 14, 15]. The composition dependence of the θ_p is presented in Fig. 4. The absolute magnitude of θ_p increases with Cr_2O_3 content for $x \geq 3$ mol %. For x > 10 mol % the slope of the increment becomes much slower, indicating weaker exchange coupling between Cr^{3+} ions, in accordance with the literature [14, 18]. The composition dependence of the molar Curie constant, C_M, is presented in Fig. 5. The values linearly vary with the Cr_2O_3 content. According to Table 1, the experimental values of the effective magnetic moment: $\mu_{eff} = (3.87 \pm 0.02)\ \mu_B$ are very close to the magnetic moment of Cr^{3+} ion in free ion state: $\mu_{Cr^{3+}} = 3.87\ \mu_B$ [19], in agreement with the values usually obtained in paramagnetic salts containing Cr^{3+} ions [19].

Table 1. Effective magnetic moments of Cr^{3+} ions in glasses from system (1).

x [mol % Cr_2O_3]	1	3	5	10	15	20
μ_{eff} [μ_B]	3.87	3.87	3.87	3.86	3.89	3.85

3.2. EPR and magnetic susceptibility studies of glasses from system (2)

EPR spectra of Fe^{3+} ions in oxide glasses generally characterized by the appearance of the resonance absorption at g ≈ 6.0, 4.27 and 2.0, their relative intensity being strongly dependent on composition [20, 21]. The g ≈ 4.27 resonance line is characteristic for isolated Fe^{3+} ions predominantly situated in rhombically distorted octahedral or tetrahedral oxygen environments [20, 21]. The g ≈ 6.0 resonance line arises from axially distorted sites. The g ≈ 2.0 resonance is assigned to those ions which interact by a superexchange coupling [21, 22].

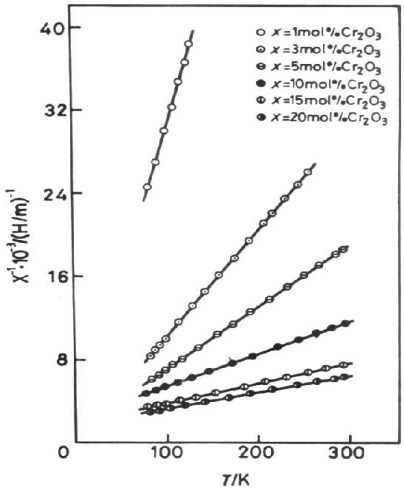

Fig. 3. Temperature dependence of the reciprocal magnetic susceptibility for glasses from system (1).

The temperature dependence of the magnetic susceptibility at high temperatures indicates an antiferromagnetic interaction between iron ions in phosphate [23], borate [24], tellurite [25] and bismuthate [26] oxide glasses. In these glasses the presence of both Fe^{3+} and Fe^{2+} ions was evidenced. The concentration range of iron over which antiferromagnetic interactions are observed depends on the glass matrix nature [27], on the preparation conditions [28] and consequently on the Fe^{3+}/Fe^{2+} ratio [20-28].

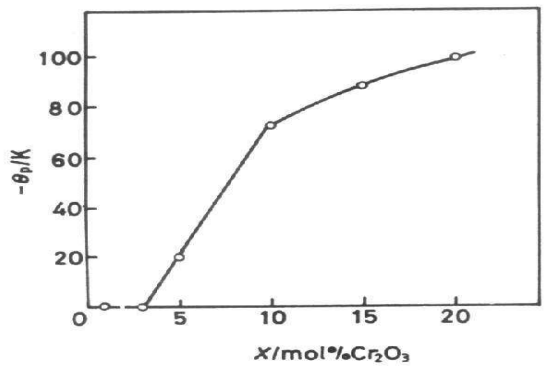

Fig. 4. The dependence of the paramagnetic Curie temperature on composition.

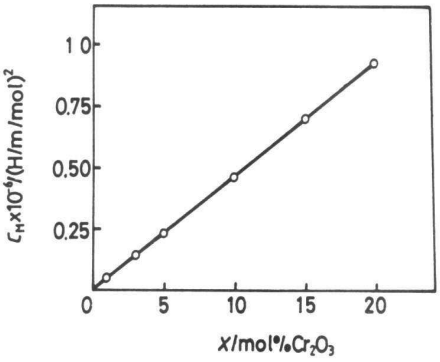

Fig. 5. The composition dependence of the molar Curie constant.

The features of the recorded EPR spectra of the Fe^{3+} ions in studied glasses are detailed in Fig. 6. The spectra consists mainly in absorption lines centered at $g \approx 4.3$ and $g \approx 2.0$, their prevalence depending on x. One also observes weak, unresolved lines centered at $g \approx 9.79$. According to [20] in rhombic vicinities, besides the transition having a $g \approx 4.3$ isotropic value corresponding to the median Kramers doublet, there are transitions corresponding to the other two doublets characterized by g factors (9.678, 0.857, 0.607) having a pronounced anisotropy. These transitions result in a large background with effective g values from 1 to 10 as reported by Griffith [29]. The existence of the $g \approx 4.3$ lines up to 5 mol % (Fig. 6) proves a predominant rhombic character of the structural units involving the Fe^{3+} ions. At low Fe^{3+} content the resonances centered at $g \approx 4.3$ prevail in the spectrum. This evolution is easier to follow if one considers the dependence of concentration on the EPR parameters, i.e. the line-height, I, the line-width, ΔH and the intensity of the absorption line, J, approximated as $J = I \cdot (\Delta H)^2$.

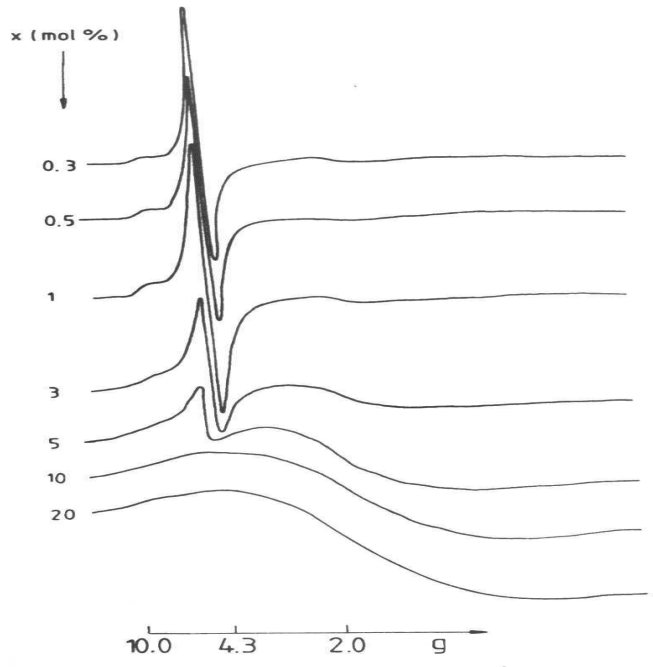

Fig. 6. EPR absorption spectra due to Fe^{3+} ions in glasses from system (2).

The concentration dependence of these parameters is plotted in Figs. 7 and 8 for the absorptions centered at $g \approx 4.3$ and $g \approx 2.0$, respectively. In contrast to the $g \approx 4.3$ resonance whose intensity increases on a narrow concentration range ($0.3 \leq x \leq 1$ mol %), then abruptly decreases and

disappears for x > 5 mol %, the g ≈ 2.0 absorptions are detectable only for x ≥ 1 mol % and their intensity constantly increases along the investigated concentration range. The restricted capacity of the glass matrix in accepting Fe^{3+} ions in structural units of well defined configuration and symmetry is typical for tellurite glasses due to particularities of their structure [18, 30]. The composition dependence of the g ≈ 2.0 absorption intensity shows an increase which does not follow linearly the Fe_2O_3 content (Fig. 8a). Over 3 mol % the iron exists in the glasses not only as Fe^{3+} but also as Fe^{2+} species. Fe^{2+} ions are not involved in the EPR absorption but their interactions with Fe^{3+} influence the characteristics of the absorption lines. According to Fig. 7b the line-width of the g ≈ 4.3 resonance increases along the investigated concentration range, but the initial slope corresponding to the dipolar broadening at low Fe^{3+} content (x ≤ 1 mol %) is changes at higher concentrations. The line-width decrease may reflect the diminishing in number of Fe^{3+} ions involved in dipole-dipole interactions due to the diminishing of these ions which participate at g ≈ 4.3 resonance (Fig. 7a). The line-width evolution of the g ≈ 2.0 resonances in Fig. 8b can be explained by having in view the cluster structure of iron which gives rise to these absorptions. There are superexchange mechanisms narrowing the absorption line balanced over a certain doping degree by broadening mechanisms due to interaction between Fe^{3+} and Fe^{2+} ions and of the disorder determined by increasing of Fe_2O_3 content.

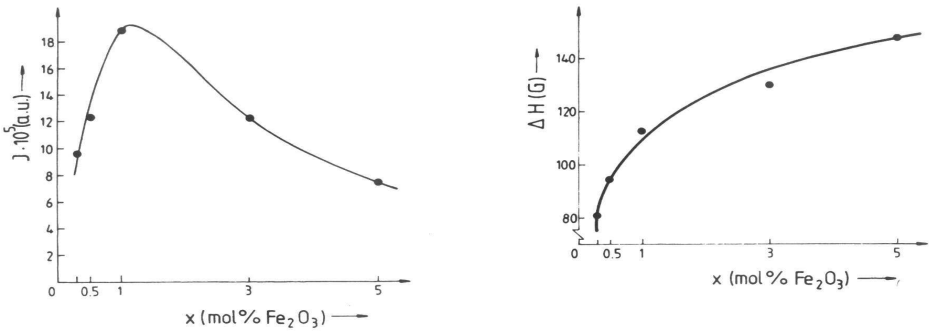

Fig. 7. The composition dependence of line intensity (a) and line-width (b) for g ≈ 4.3 resonance.

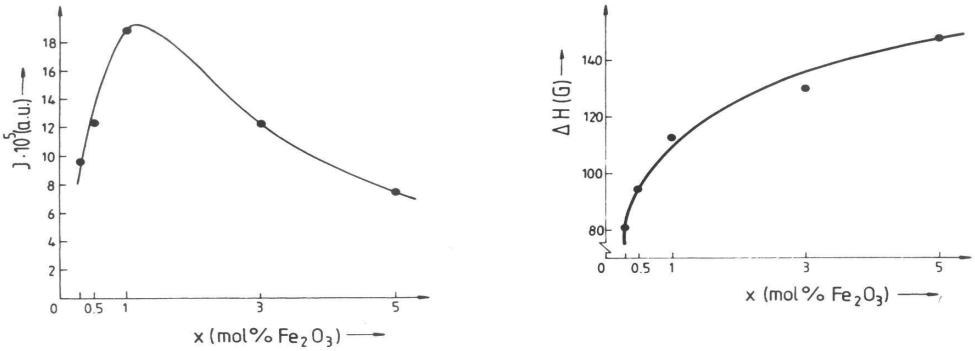

Fig. 8. The composition dependence of line intensity (a) and line-width (b) for g ≈ 2.0 resonance.

The $\chi^{-1} = f(T)$ of some glasses from the investigated system are studied. For the glasses with x ≤ 1 mol % the Curie law is evidenced. For x > 1 mol % the $\chi^{-1} = f(T)$ obey a Curie-Weiss behaviour with $\theta_p < 0$, which denotes the iron ions are predominantly antiferomagnetically coupled. Therefore, in these glasses the iron ions behave magnetically similar as in other oxide glasses [23-26]. The absolute magnitude of θ_p values increases for x > 1 mol % (Table 2). This fact indicates that the exchange interactions increase with the concentration of iron ions [18]. The experimental C_M values for x > 1 mol % are lower than the expected ones, assuming that all iron ions are in Fe^{3+} valence state and higher than those characteristic for Fe^{2+} ions (Table 2). In this way we suppose for the glasses

with x > 1 mol % both Fe^{3+} and Fe^{2+} ions to be present. The presence of Fe^{3+} ions was evidenced in all investigated glasses by EPR studies. The Fe^{2+} valence state of iron ions may be favored by the presence of the Te^{4+} ions in the glasses. In this case, having in view the magnetic moment values of free Fe^{3+} and Fe^{2+} ions: $\mu_{Fe^{3+}} = 5.92\,\mu_B$ and $\mu_{Fe^{2+}} = 4.90\,\mu_B$ [19], we can estimate in first approximation the molar fraction of these ions by using the relations:

$$x\mu_{eff}^2 = x_1\mu_{Fe^{3+}}^2 + x_2\mu_{Fe^{2+}}^2 \text{ and } x = x_1 + x_2, \quad (1)$$

where $\mu_{eff} = 2.827\ (C_M/2x)^{1/2}$ are experimental effective magnetic moments, x_1 and x_2 are molar fraction of iron ions in Fe^{3+} and Fe^{2+} valence states (Table 2). One can observe from these data that in the investigated glass system the molar fraction of Fe^{2+} ions are higher than that of Fe^{3+} ones for $x \geq 3$ mol %. One also remark that in the glass with x = 1 mol % only Fe^{3+} ions are present. The intensity of the absorption line centered at $g \approx 2.0$ due Fe^{3+} species, does not follow the impurifying degree of the samples because as x > 1 mol % iron occurs in the sample as Fe^{2+} ions too, their weight becomes even higher than that of Fe^{3+} ions. Having in view these results, the data for glasses containing more that 1 mol % Fe_2O_3 can be explained by accepting the existence of the Fe^{2+}-Fe^{2+}, Fe^{3+}-Fe^{3+}, Fe^{2+}-Fe^{3+} exchange pairs.

Table 2. θ_p, C_M and molar fraction of the Fe^{3+} and Fe^{2+} ions in glasses from system (2).

x [mol % Fe_2O_3]	θ_p [K]	C_M [emu/mol]	x_1 [mol % $Fe_2^{3+}O_3$]	x_2 [mol % $Fe_2^{2+}O_3$]
1	0	0.0811	1	-
3	-30	0.2211	1.4	1.6
5	-46	0.3620	2	3
10	-72	0.7220	4	6
20	-100	1.4720	8.4	11.6

3.3. EPR and magnetic susceptibility studies of glasses from system (3)

In oxide vitreous systems containing manganese, the EPR spectra are due to the Mn^{2+} ions. In order to explain them, the structural characteristics of boro-tellurite matrices, and the previous data on EPR of Mn^{2+} ions in borate [8, 31] and tellurite [32] glasses were taken into account. In borate glasses the Mn^{2+} ions were detected in highly symmetric vicinities and show intense absorption at $g \approx 2.0$ having the hyperfine structure (hfs) very well resolved for low MnO content [8]. The $g \approx 4.3$ absorption is small and broad, and has unresolved hfs. In tellurite glasses with low Mn^{2+} ions content we detected an intense absorption at $g \approx 4.3$ which have hfs very well resolved and broad unresolved resonances at $g \approx 2.0$ [32]. In oxide glasses the hfs of $g \approx 4.3$ absorption was detected only in a few cases [31, 32].

The magnetic susceptibility data were reported for the phosphate [3], borate [34] tellurite [35] and bismuthate [36] glasses containing manganese ions. In some of these glasses only the Mn^{2+} ions [9, 31, 32, 34] were detected. In the papers [35, 37], we have shown that in some borate glass matrices, both Mn^{2+} and Mn^{3+} ions are present.

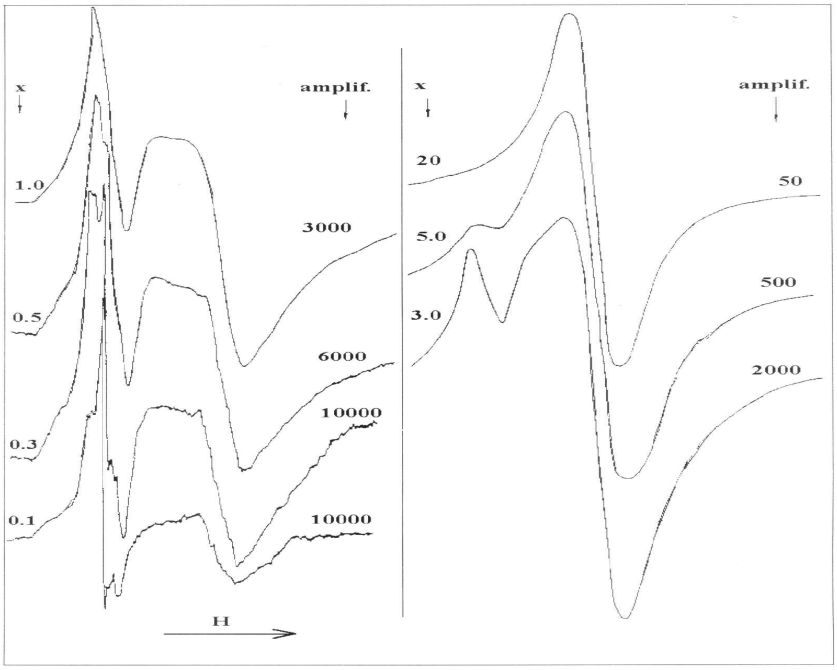

Fig. 9. EPR absorption spectra due to Mn^{2+} ions in glasses from system (3).

The recorded EPR spectra of the studied glasses are presented in Fig. 9. The spectra are complex ones in the low concentration range of MnO and become simpler, down to a single absorption line, for glasses with high manganese content. For x < 5 mol % the EPR spectrum consists in absorption lines centered at g ≈ 4.3 and g ≈ 2.0 values. The hfs were resolved on both g ≈ 4.3 and g ≈ 2.0 absorptions due to the nuclear spin (I = 5/2) interaction (Fig. 10).

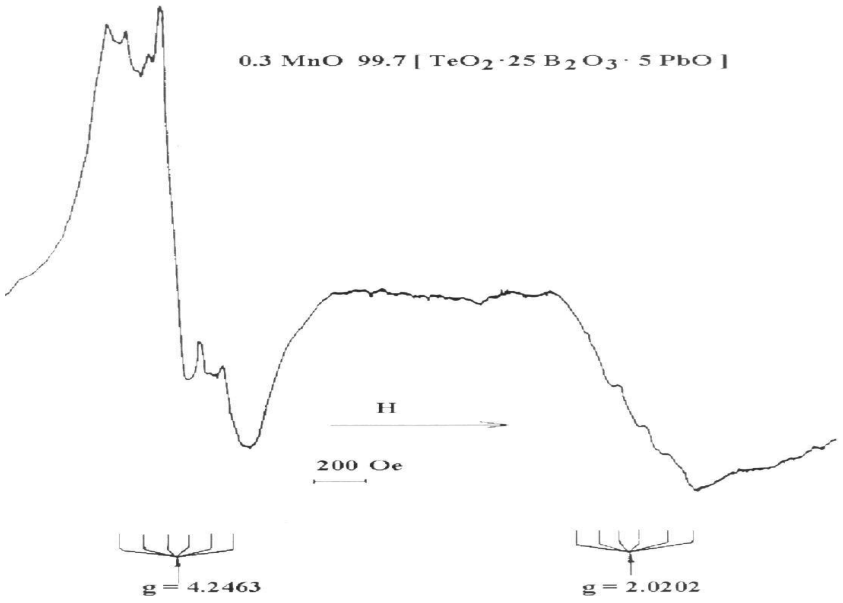

Fig. 10. EPR absorption spectrum for x = 0.3 mol % that reveals the hfs characteristic of Mn^{2+} ions.

The EPR parameters ΔH anf J evolution as function of the MnO content are illustrated in Figs. 11, 12 and 13. For g ≈ 4.3 absorption the line-width and intensity increase along the x ≤ 1 mol %, then abruptly decrease. For g ≈ 2.0 absorption the line-width has an abrupt increase on the x ≤ 1 mol %, and then narrowing of the signal until 20 mol % and again a slow broadening for x > 20 mol %. The intensity of this line increases in studied glasses, but attenuates for x > 20 mol % (Fig. 13). At low concentration of paramagnetic ions the absorption is a superposition of contributions from Mn^{2+} ions involved in tellurite and borate rich phases. In case of g ≈ 2.0 absorptions for x ≤ 1 mol % the line broadene as result of dipolar interactions between manganese ions. For x > 1 mol % this broadening is stopped by the exchange narrowing, especially for x ≤ 5 mol %. For x > 20 mol % the broadening of the g ≈ 2.0 absorption line can be explained by the increased role of the Mn^{3+} ions and of the disorder determined by the increase of the MnO content.

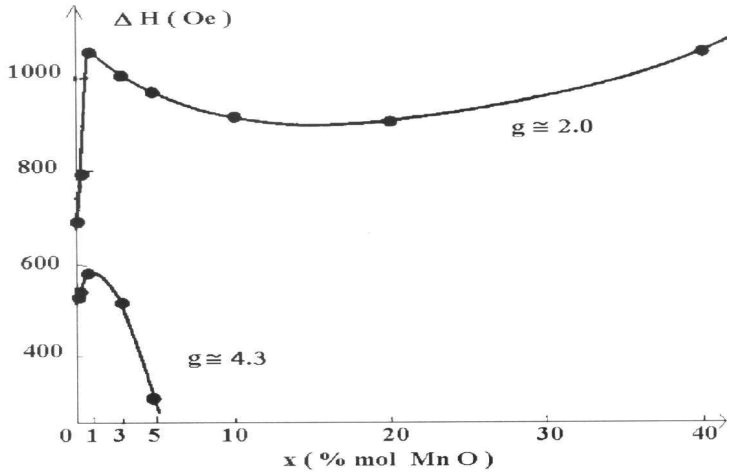

Fig. 11. The line-width evolution of the EPR absorptions.

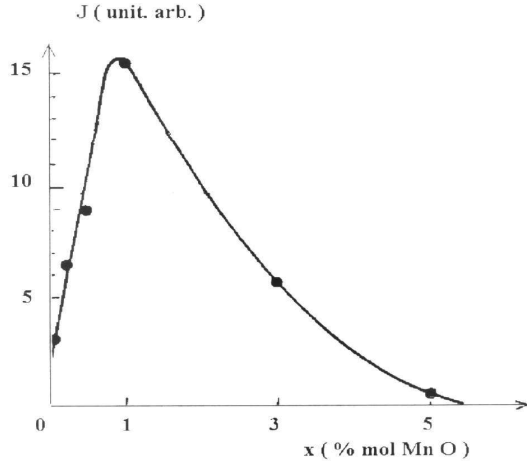

Fig. 12. The variation of the g ≈ 4.3 absorption line intensity with MnO concentration.

The $\chi^{-1} = f(T)$ of these glasses were studied. For x ≤ 1 mol % a Curie law is observed, but for higher MnO content these dependencies obey a Curie-Weiss behaviour with $\theta_p < 0$, the manganese ions being antiferromagnetically coupled [33]. The absolute magnitude of the θ_p values increases for x > 1 mol % (Table 3). The composition dependence of the C_M is shown in Table 3. For glasses with x ≥ 10 mol %, the experimental values of the C_M are lower than those corresponding of the MnO content, considering that all manganese ions are in the Mn^{2+} valence state and higher than those characteristic for Mn^{3+} ions. The presence of Mn^{2+} ions was evidenced by EPR in all investigated glasses. The Mn^{3+} valence states can be favoured by the presence of the Te^{4+} and Pb^{2+} ions in the

glasses. Then, using the $\mu_{Mn^{2+}} = 5.92\,\mu_B$ and $\mu_{Mn^{3+}} = 4.90\,\mu_B$ for free ions state [19], we estimate in a first approximation the molar fractions of these ions in studied glasses by considering the relations (1), where $\mu_{eff} = 2.827\,(C_M/x)^{1/2}$. The results are presented in Table 3. These data show that the molar fraction of Mn^{2+} ions increases up to 40 mol % and the molar fraction of Mn^{2+} ions is higher than that of Mn^{3+} ions.

Table 3. θ_p, C_M and molar fraction of the Mn^{2+} and Mn^{3+} ions in glasses from system (3).

x [mol % MnO]	θ_p [K]	C_M [emu/mol]	x_1 [mol % $Mn^{2+}O$]	x_2 [mol % $Mn^{3+}O$]
0.5	0	0.02198	0.5	0
3	-3.8	0.1301	3	0
5	-7	0.2124	5	0
10	-15	0.4323	9.7	0.3
20	-32.5	0.8130	15.6	4.4
40	-67.5	1.5315	24.3	15.7

3.4. EPR and magnetic susceptibility studies of glasses from system (4)

EPR studies of Cu^{2+} ions have been performed by many authors [38-40] in some oxide glasses. In their papers the concentration effect of some network-former and network –modifier oxides on the spin-Hamiltonian parameters and ligand field absorption energies have been studied.

Juza et al. [41] reported magnetic investigations performed on copper-sodium-borate glasses. The copper phosphate glasses show an antiferromagnetic behaviour [42]. We have investigated the valence states and distribution of copper in various glass matrices [43-45]. In some of these glasses the copper ions are in divalent state [43, 44], but in others the ions are in Cu^{+} and Cu^{2+} valence states [45]. Also in some of these glasses [44, 45], the Cu^{2+} ions experience negative superexchange interactions.

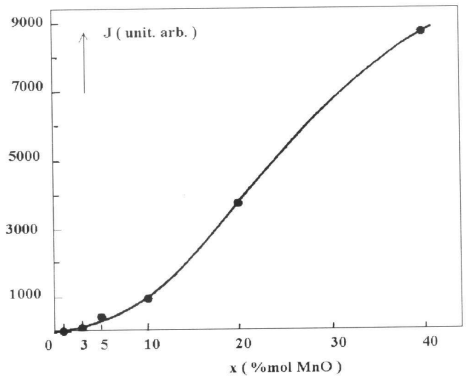

Fig. 13. The variation of the g ≈ 2.0 absorption line intensity with the MnO concentration.

For studied glasses, the EPR spectra of Cu^{2+} ions show a strong dependence on the CuO content (Fig. 14). For x ≤ 5 mol % the EPR spectra are asymmetric, characteristic for isolated or those participating at the dipolar interactions of Cu^{2+} ions in an axially distorted octahedral environment [44]. The spectra show the parallel partially resolved hfs due to the interaction of the unpaired electron with the nuclear spin I = 3/2 of the Cu^{2+} ion. The perpendicular hfs is not resolved indicating a width of the individual components exceeding the $|A_\perp|$ separation. As the concentration of CuO rises (x ≤ 3 mol %), the parallel hfs becomes less resolved due to peak broadening effect.

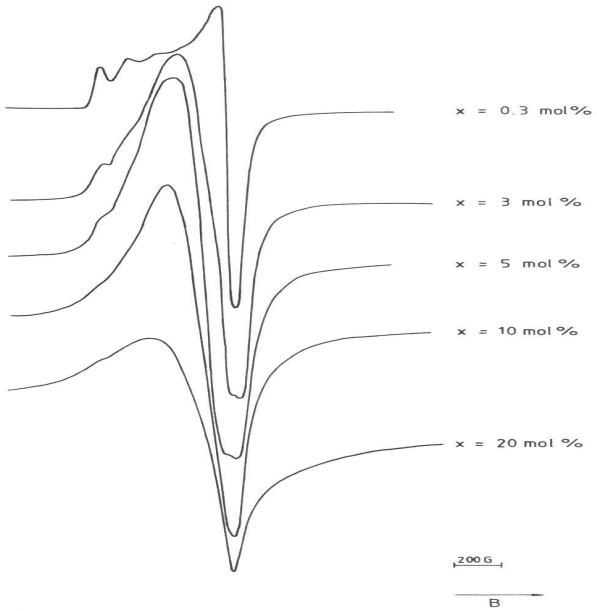

Fig. 14. EPR spectra due to Cu^{2+} ions in glasses from system (4).

The fluctuations of the ligand involving Cu^{2+} ions broaden progressively the absorption lines so that hfs is rapidly smeared. At about 3 mol % a large absorption due to clusters of Cu^{2+} ions superimposes the spectrum characteristic for ions not participating to exchange interactions. The axial environment of the Cu^{2+} ions is destroyed and the absorption line becomes more symmetric proving a higher degree of disorder in glasses. In the high concentration range ($x \geq 10$ mol %) the absorption spectrum reduces to a single, slightly asymmetric line. The spectra are similar to those reported for some copper containing oxide glasses [43, 45] and differ from other [38, 44]. For the last glasses, resolved hfs appear in both parallel and perpendicular bonds. The $g \approx 2.2$ resonance line-width (Fig. 15) increases up to 20 mol %, where a change of slope takes place. Following [43] at small concentration the increase of line-width is due to the dipolar interactions. For higher concentrations ($x \geq 20$ mol %) the increase of line-width is attenuated and this supports the existence of exchange interaction between Cu^{2+} ions [43, 45]. The modification of EPR spectra with the increasing of CuO content are explained supposing that they are the result of the superposition of two EPR absorptions, one showing the hfs typical for not participating to exchange interactions of Cu^{2+} ions and other consisting of a line centered at $g \approx 2.2$ typical for the clustered Cu^{2+} ions ($x \geq 20$ mol %).

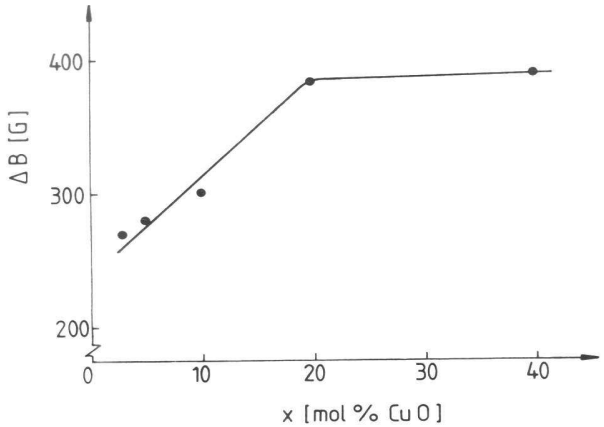

Fig. 15. The compositional dependence of the line-width for the $g \approx 2.2$ resonance.

The χ^{-1} = f(T) for these glasses have been also studied. For x ≤ 10 mol % the χ^{-1} vs T follows a Curie law and for higher CuO content the glasses obey a Curie-Weiss type dependence with $\theta_p < 0$. At temperatures below 25 K and for x > 20 mol %, the curve χ^{-1} = f(T) deviates from a linear dependence. This dependence cannot be ascribed to an increase of χ as due to the presence of a magnetic ordered phase, since this contribution was subtracted when the χ values were determinated. According to the assumption of Simpson [48] an unusual downward curvature of the χ^{-1} for decreasing temperature was predicted. Our studies show that the χ^{-1} = f(T) was in agreement with the theoretical model [48]. The composition dependence of θ_p indicates that for x > 10 mol % the absolute magnitude is increasing when CuO content increases (Table 4). The magnetic properties of these glasses are due to both dipolar and exchange interactions between Cu^{2+} ions, their relative number being dependent on composition. The features of the EPR spectra are consistent with the results of magnetic measurements. The values of the C_M are presented in Table 4. In the case of the glasses with x ≤ 10 mol %, the experimental magnetic moment $\mu_{eff} = (1.73 \pm 0.03)\ \mu_B$ is very close to the magnetic moment of the Cu^{2+} free ion: $\mu_{Cu^{2+}} = 1.73\,\mu_B$ [19]. The experimental value of μ_{eff} indicates that the copper ions are present in octahedral coordination [49], in agreement with the EPR investigations. The C_M and μ_{eff} for the glasses with x > 10 mol % are lower than those considering that all copper ions are in Cu^{2+} valence state. Therefore, both Cu^{2+} and Cu^{+} ions are present in glasses, the last one being diamagnetic. In this case, having in view the value of the $\mu_{Cu^{2+}}$ for the free ion state, we have estimated the molar fraction of Cu^{2+} ions (denoted by y, Table 4) by using relation $y = 2.827^2\ C_M/\mu^2_{Cu^{2+}}$. Table 4 shows that for x ≥ 20 mol % only 60-70 % of copper ions are in a divalent state.

Table 4. θ_p, C_M, μ_{eff} and the Cu^{2+} content in glasses from system (4).

x [mol % CuO]	θ_p [K]	C_M [emu/mol]	μ_{eff} [μ_B]	J [mol % CuO]
5	0	0.01879	1.73	5
10	0	0.03878	1.76	10
20	-3	0.04496	-	12
40	-20	0..10544	-	28.2

4. Conclusions

The homogeneous tellurite glasses with chromium, iron, manganese and copper ions are formed in determined range concentrations, which depend of the nature of transition metal ions.

EPR and magnetic susceptibility data show that the local neighbourhoods, structural distributions, valence states and strength of magnetic interactions depend of the nature and concentration of transition metal ions.

References

[1] N. Ovcharenko, A.Yakhkind, Opt. Mech. Prom. **3**, 47 (1968).
[2] M. Weber, J. Meyers, D. Blackurn, J. Appl. Phys. **52**, 2944 (1981).
[3] J. Koen, M. Res, R. Heckroodt, V. Hasson, J. Phys. D: Appl. Phys. **9**, L13 (1976).
[4] H. Harper, P. F. James, P. W. McMillan, Discuss Faraday Soc. **50**, 382 (1970).
[5] J. Moncoujoux, J. Faurier, J. Kohlmuller, Verres Refract. **31**, 405 (1977).
[6] M. E. Lines, J. Appl. Phys. **69**, 6876 (1991).

[7] E. Burzo, Fizica fenomenelor magnetice (roum.), Physics of Magnetic Phenomena, Ed. Academiei, Bucuresti, vol. I, 1979, p.79.
[8] R. J. Landry, J. T. Fournier, C. G. Young, J. Chem. Phys. **46**, 1285 (1967).
[9] D. Loveridge, S. Parke, Phys. Chem. Glasses, **12**, 19 (1971).
[10] G. Fuxi, D. He, L. Huiming, J. Non-Cryst. Solids **52**, 135 (1982).
[11] A. S. Rao, J. L. Rao, J. S. V. Lakshman, Solid State Commun. **85**(6), 529 (1993).
[12] I. Ardelean, M. Peteanu, S. Filip, V. Simon, C. Bob, J. Mat. Sci. **13**, 374 (1997).
[13] I. V. Chepeleva, E. R. Zhilinskaya, V. V. Lazukin, A. P. Cernov, phys. status solidi B **73**, 65 (1975).
[14] I. Ardelean, Gh. Ilonca, M. Peteanu, D. Barbos, E. Indrea, J. Mat. Sci. **17**, 1988 (1982).
[15] O. Cozar, I. Ardelean, I. Bratu, Gh. Ilonca, S. Simon, Solid State Commun. **86**, 569 (1993).
[16] J. Wong, C. A. Angell, Appl. Spectr. Res. **4**(2), 155 (1971).
[17] C. M. Hurd, Contemp. Phys. **23**, 469 (1982).
[18] E. J. Friebele, N. C. Koon, L. K. Wilson, D. L. Kinser, J. Amer. Ceram. Soc. **57**, 237 (1974).
[19] E. Burzo, Fizica Fenomenelor Magnetice (roum.), Physics of Magnetic Phenomena, Ed. Academiei, Bucharest, vol. **1**, 1979, p. 241.
[20] H. H. Wickman, M. P. Klein, D. A. Sirley, J. Chem. Phys. **42**, 2113 (1965).
[21] E. Burzo, I. Ardelean, Phys. Status Solidi B **87**, K137 (1978).
[22] D. W. Moon, M. J. M. Aitken, R. K. Maccrone, G. S. Cieloszky, Phys. Chem. Glasses **16**, 91 (1975).
[23] B. Kumar, C. H. Chen, J. Appl. Phys. **75**, 6760 (1994).
[24] E. Burzo, I. Ardelean, Phys. Chem. Glasses **20**, 15 (1979).
[25] I. Ardelean, Gh. Ilonca, M. Peteanu, I. Luca, Studia Univ. Babes-Bolyai, Physica **1**, 65 (1979).
[26] I. Ardelean, Gh. Ilonca, O. Cozar, V. Simon, S. Filip, Mat. Lett. **21**, 321 (1994).
[27] E. Burzo, I. Ardelean, I. Ursu, J. Mat. Sci. **15**, 58 (1980).
[28] E. Burzo, I. Ursu, D. Ungur, I. Ardelean, Mat. Res. Bull. **15**, 1273 (1982).
[29] J. S. Griffith, Molec. Phys. **8**, 213 (1964).
[30] G. Sperlich, P. Urban, Phys. Status Solidi B **61**, 475 (1974).
[31] J. W. H. Shreurs, J. Chem. Phys. **69**, 2151 (1978).
[32] I. Ardelean, M. Peteanu, Gh. Ilonca, phys. status solidi A **58**, 433 (1986).
[33] E. J. Friebele, L. K. Wilson, A. W. Dozier, D. L. Kinser, phys. status solidi B **45**, 323 (1971).
[34] C. J. Schinkel, G. W. Rathenau, Physics of Non-Crystalline Solids, North Holland, Amsterdam, 1965, p. 215.
[35] I. Ardelean, Gh. Ilonca, M. Peteanu, Solid State Commun. **52**, 147 (1984).
[36] I. Ardelean, M. Peteanu, S. Filip, V. Simon, I. Todor, Solid State Commun. **105**, 339 (1998).
[37] I. Ardelean, Gh. Ilonca, O. Cozar, Rev. Roum. Phys. **33**, 179 (1988).
[38] H. Hosono, H. Kawazoe, T. Kavazawa, J. Non-Cryst. Solids **34**, 339 (1979).
[39] O. Cozar, I. Ardelean, J. Non-Cryst. Solids **92**, 279 (1987).
[40] A. S. Rao, J. L. Rao, S. V. J. Laksman, J. Chem. Phys. Solids **53**, 24 (1992).
[41] R. Juza, H. Seidel, J. Tiedemann, Angew. Chem. **78**, 41 (1966).
[42] R. Egami, O. S. Sacli, A. W. Simpson, A. L. Terry, Amorphous Magnetism, Plenum Press, New York, 1973, p. 27.
[43] I. Ardelean, Gh. Ilonca, M. Peteanu, J. Non-Cryst. Solids **51**, 389 (1982).
[44] I. Ardelean, M. Coldea, O. Cozar, Nucl. Insttum. Methods **199**, 189 (1982).
[45] I. Ardelean, O. Cozar, Gh. Ilonca, Solid State Commun. **50**, 87 (1984).
[46] H. Kawazoe, H. Hosono, H. Hokumai, J. Non-Cryst. Solids **40**, 291 (1980).
[47] C. Kittel, E. Abrahams, Phys. Rev. **90**, 238 (1953).
[48] A. W. Simpson, phys. status solidi **40**, 207 (1970).
[49] M. Leventhal, P. J. Bray, Phys. Chem. Glasses **6**, 113 (1965).